Intrinsic defect formation in amorphous SiO_2 by electronic excitation: Bond dissociation versus Frenkel mechanisms

Koichi Kajihara,[1,2,*] Masahiro Hirano,[1] Linards Skuja,[1,3] and Hideo Hosono[1,4]

[1]*Transparent Electro-Active Materials Project, ERATO-SORST, Japan Science and Technology Agency, in Frontier Collaborative Research Center, Mail Box S2-13, Tokyo Institute of Technology, 4259 Nagatsuta, Midori-ku, Yokohama 226-8503, Japan*

[2]*Department of Applied Chemistry, Graduate School of Urban Environmental Sciences, Tokyo Metropolitan University, 1-1 Minami-Osawa, Hachioji 192-0397, Japan*

[3]*Institute of Solid State Physics, University of Latvia, Kengaraga iela 8, LV1063 Riga, Latvia*

[4]*Materials and Structures Laboratory & Frontier Collaborative Research Center, Tokyo Institute of Technology, 4259 Nagatsuta, Midori-ku, Yokohama 226-8503, Japan*

(Received 5 August 2008; published 16 September 2008)

Two competing mechanisms of intrinsic defect formation in amorphous SiO_2 (a-SiO_2), i.e., the vacancy-interstitial (Frenkel) mechanism and Si-O bond dissociation to form silicon and oxygen dangling bonds, were compared under γ-ray electronic excitation. The Frenkel mechanism was found to be dominant. The concentrations of both kinds of defects strongly correlate with the degree of the structural disorder of a-SiO_2, providing experimental evidence that both types of intrinsic defect pairs are formed mainly from the strained Si-O-Si bonds. The bond dissociation mechanism is more susceptible to the structural disorder than the vacancy-interstitial mechanism.

DOI: 10.1103/PhysRevB.78.094201 PACS number(s): 78.30.Ly, 61.72.J−, 78.40.−q, 78.55.Qr

I. INTRODUCTION

The decay of electronic excitation may result in the formation of intrinsic point defects in solids.[1] The intrinsic defect formation in amorphous SiO_2 (a-SiO_2) has been studied extensively both experimentally[2–13] and theoretically[14–17] because of its fundamental interest and significance in various SiO_2-based devices including ultraviolet (UV) optics, optical fibers, and gate dielectric films. The structural disorder that distinguishes amorphous from crystalline states may provide additional channels of defect formation; understanding these channels is important for both the applications and general science of the amorphous state.

Two major intrinsic defect processes are known for a-SiO_2. The first one, peculiar to the amorphous state, is the cleavage of a single Si-O bond forming a silicon and oxygen dangling-bond pair : $\equiv Si^{\bullet}$ (E' center) and $\equiv SiO^{\bullet}$ [nonbridging oxygen hole center (NBOHC)],[2–7,17]

$$\equiv \text{Si-O-Si} \equiv \xrightarrow{h\nu} \equiv Si^{\bullet} + {}^{\bullet}OSi \equiv . \quad (1)$$

This reaction is enhanced by high-pressure densification[2,18] or high-temperature annealing[5,7] treatments, which increase the concentration of "strained" Si-O-Si bonds,[2–4,6,7,19] having Si-O-Si bonding angles largely different from the relaxed angle ($\sim 140° - 150°$). There is evidence[1,18,20,21] that static potential fluctuations associated with the strained bonds enhance the self-trapping of radiation-induced holes and excitons. Indeed, in α-quartz, a crystalline polymorph of SiO_2 where all Si-O-Si bonds are equally relaxed ($\sim 144°$), excitons can be self-trapped only transiently[22–24] and holes are unlikely to be self-trapped[22] even at low temperatures. Furthermore, dangling-bond formation by mechanism [Eq. (1)] has not been confirmed in electronically excited α-quartz.[25] Thus, it is generally considered that the strained Si-O-Si bonds are the main source of the dangling bonds. However, in real glasses this intrinsic mechanism is often obscured by extrinsic ones: the creation of dangling bonds by the decomposition of SiH,[26,27] SiOH,[28–31] or SiCl (Refs. 4 and 32) groups, present in most types of synthetic a-SiO_2.

An alternative mechanism is the displacement of a bridging oxygen atom to form an interstitial oxygen atom (O^0) and the vacancy (Si-Si bond),[8–11,14,15]

$$\equiv \text{Si-O-Si} \equiv \xrightarrow{h\nu} \equiv \text{Si-Si} \equiv + O^0. \quad (2)$$

Equation (2) is similar to the Frenkel mechanism in crystalline solids.[1] However, its efficiency in a-SiO_2 may depend on the degree of the structural disorder, and this effect has yet to be proven. Its examination has been difficult because electron paramagnetic resonance (EPR), historically the most effective tool in studying the defect processes in a-SiO_2,[2–6,8,9,12,33] is silent for diamagnetic Si-Si bonds and O^0. Besides, the characteristic 7.6 eV optical-absorption (OA) band of Si-Si bond[13,34–39] is inaccessible to conventional visible-UV spectrometers. Furthermore, because interstitial O^0 does not have a distinct spectroscopic signature, its creation has to be detected indirectly through reactions involving O^0, such as the formation of peroxy radicals (POR) ($\equiv SiOO^{\bullet}$) (Refs. 8 and 40) and interstitial oxygen molecules (O_2).[9–11] Thus, the mechanism of Eq. (2) is still largely unexplored, and it remains unclear which of Eqs. (1) and (2) is the main mechanism.

In the preceding communication[41] we compared the efficiency of the two intrinsic mechanisms [Eqs. (1) and (2)] in a-SiO_2 by simultaneously detecting all the products (E' center, NBOHC, Si-Si bond, and interstitial O_2) by optical means, and reported that Eq. (2) is dominant over Eq. (1). In this paper we extended the study for samples annealed at different temperatures to examine the influence of the degree of structural disorder of a-SiO_2. Fluorine-doped synthetic a-SiO_2 was chosen because fluorine doping helps to elimi-

nate extrinsic defect precursors including SiOH, SiCl, and SiH groups. Furthermore, fluorine, which forms a strong Si-F bond in a-SiO_2, hardly participates in radiation-induced defect processes[4,42,43] and does not obscure intrinsic mechanisms. A ^{60}Co γ ray source was used to homogeneously ionize samples while avoiding the elastic displacive collisions,[1,44] with dose range extended as compared to the preceding work.[41]

II. EXPERIMENTAL PROCEDURE

A. Sample preparation and measurements

Two types of fluorine-doped a-SiO_2 were used:[45] "DryF" (SiF $\sim 4\times10^{19}$ cm^{-3}, SiOH $\lesssim 10^{17}$ cm^{-3}), having the lowest concentration of the extrinsic defect precursors, and "WetF" (SiF $\sim 1.4\times10^{19}$ cm^{-3}, SiOH $\sim 1\times10^{18}-2\times10^{18}$ cm^{-3}). The WetF sample was employed to test the influence of SiOH groups, which are common extrinsic defect precursors each radiolyzed to an NBOHC and a mobile interstitial hydrogen atom.[28–31] The sample size was $10\times6.5\times2$ mm^3 and the two largest faces were polished to an optical finish. Samples with different distributions of Si-O-Si angles were prepared by varying the preannealing temperature. First, all specimens were thermally equilibrated at 900 °C for 120 h. Since this annealing was relatively long, it was performed in a vacuum to avoid incorporation of gas molecules that may influence the radiation-induced defect processes. Then, part of each specimen set was additionally heated for 10 min at 1400 °C in air and quenched to room temperature. All samples were then irradiated with ^{60}Co γ rays with an absorbed dose rate of $\sim1.3\times10^4$ Gy h^{-1} (SiO_2 equivalent).[46] The induced OA was measured by visible-UV and vacuum-UV spectrometers (U-4000, Hitachi, and VU-201, Bunkou-Keiki). Interstitial O_2 created by the dimerization of O^0 was detected by characteristic infrared (IR) photoluminescence (PL) at 1272 nm using a Fourier-transform IR Raman spectrometer (Model 960, Nicolet). The relative O_2 concentrations were evaluated from the PL intensity under 765 nm excitation[10] and were converted to absolute concentrations using a reference sample with a known O_2 concentration.[47]

B. Accuracy of the defect concentration estimates

In this study, the concentrations of Si-Si bond, E' center, and NBOHC were evaluated from the intensity of their characteristic OA bands, and the concentration of interstitial O_2 was determined from the intensity of the IR PL band. Thus, it is very important to estimate the accuracy of the coefficients that correlate the OA and PL band intensities with the concentration of relevant defect species.

The concentration of Si-Si bond was calculated from the intensity of the 7.6 eV OA band using the absorption cross section $\sigma=7.5\times10^{-17}$ cm^2, corresponding to the oscillator strength $f\simeq0.4$.[48] The σ value was experimentally determined[38] relying on the reaction

$$\equiv \text{Si-Si} \equiv + \text{H}_2 \rightarrow \equiv \text{SiH} + \text{HSi} \equiv , \qquad (3)$$

where the concentration change of SiH groups were evaluated using σ of their IR absorption band at 2260 cm^{-1}.[49] The experimentally obtained f value agrees well with the value ($f\simeq0.3$) predicted by an *ab initio* calculation.[50] Furthermore, Si_2H_6, the simplest molecule containing Si-Si bond, exhibits an OA band at 7.6 eV and its σ value (6×10^{-17} cm^2) is also close to σ of Si-Si bond in a-SiO_2.[51] This observation is consistent with the theoretical indications[35,50,52,53] that the 7.6 eV OA band originates from the electronic transition from the bonding σ state to antibonding σ or Rydberg states of Si-Si bond, suggesting that the transition is insensitive to functional groups outside of the Si-Si bond. The uncertainty in σ of the 7.6 eV band determined in Ref. 38 arises mainly from that of σ of the 2260 cm^{-1} band of SiH group, where $\sim$20% difference still remains for values reported so far.[49,54,55]

The concentration of E' center was evaluated from the intensity of the 5.8 eV OA band.[56] Since E' center is paramagnetic, σ of this band can be directly determined by measuring the concentration of unpaired spins. A good linear relation has been found between the intensity of the 5.8 eV OA band and the concentration of the unpaired spins, determined by the magnetic-susceptibility measurement,[57] the conventional EPR technique,[57–59] and the spin-echo decay.[60] The calculated σ in units of 10^{-17} cm^2 are 3.4 ± 1,[57,61] 2,[58,62] 3.2,[60] and 3.1 ± 2.[59,63] In the present study we employed a value of $\sigma=2.5\times10^{-17}$ cm^2. A theoretical calculation has predicted two OA bands of $f=0.3$ at 5.8 eV and $f=0.03$ at 5.9 eV.[64] The former value corresponds to 4×10^{-17} cm^2,[48] which is close to the experimental values.

The concentration of NBOHC was determined from the intensity of the 4.8 eV OA band. In principle, σ of this OA band could be obtained from the concentration of the unpaired spins because NBOHC is paramagnetic as well. However, the correlation between OA and EPR signals of NBOHC is less straightforward. A serious problem is occasional presence of "EPR-silent" NBOHC; unlikely to the conventional NBOHCs,[65] EPR-silent NBOHCs do not give measurable EPR signals around $g=2$,[66–68] making it difficult to accurately measure the concentration of NBOHC by EPR. Such NBOHCs can be formed when the ground state is degenerated and the momentum of the unpaired spin is combined with the angular momentum of the degenerated oxygen $2p\pi$ orbitals.

NBOHC exhibits another weak but distinct OA band at 1.95 eV, which is accompanied by a nearly resonant PL band at 1.9 eV. The electron-phonon coupling of the electronic transition responsible for these OA and PL bands is very small. This allows σ of the 1.95 eV OA band to be evaluated from the time decay of the PL intensity, offering a unique opportunity to determine σ of OA bands of NBOHC solely by optical means. An f value of 1.55×10^{-4} has been derived provided that the PL decay constant of the 1.9 eV PL band is 20 μs.[69] However, a very recent study has reported that the PL decay constant is smaller (15.3 ± 0.3 μs), resulting in an increase in f and σ.[70] We tentatively set the PL decay constant as 18 μs,[71] and obtain σ of 9.5×10^{-20} cm^2 for the 1.95 eV OA band.[48] The peak cross section of the much stronger 4.8 eV OA band of NBOHC is then obtained as $\sigma\simeq4.9\times10^{-18}$ cm^2 by multiplying with the ratio of the peak amplitudes of the 1.95 and 4.8 eV OA bands ($\sim$52), which is easily measured in a-SiO_2 with large NBOHC concentration.[72,73]

TABLE I. Peak position, peak absorption cross section, and Gaussian FWHM of optical-absorption bands of color centers used for the peak decomposition and concentration evaluation in this study. The source and uncertainty of the peak absorption cross section, which are crucial in evaluating the concentration, are described in Sec. II B.

	NBOHC	Divalent Si	E' center	Si-Si
Peak position (eV)	4.8	5.05	5.78	7.6
Peak absorption cross section (10^{-18} cm^2)	4.9	47[a]	25	75
Gaussian FWHM (eV)	1.07	0.3	0.8	0.7

[a]Used only for crude concentration evaluation of divalent Si.

Divalent Si (-$\ddot{\text{S}}$i-) is not a product of reactions [Eqs. (1) and (2)]. However, the 5.0 eV OA band of divalent Si was considered because this band overlaps, often as a minor component, with the 4.8 eV band of NBOHC and the 5.8 eV band of E' center. The 5.0 eV band of divalent Si appears as an isolated peak in an unirradiated oxygen-deficient a-SiO_2,[37,74] and the peak position and full width at half maximum (FWHM) are well known. Furthermore, since divalent Si is a photoluminescent center, the PL excitation measurement of the singlet and triplet PL bands (4.4 and 2.7 eV, respectively) as well reproduces the peak shape of the 5.0 eV OA band.[37,74–76] The σ value of the 5.0 eV OA band, calculated from the PL decay constant of the 4.4 eV singlet PL band ($\sim$4 ns), was $\sim 4.7\times10^{-17}$ cm^2 ($f\simeq0.135$).[48,69] Nevertheless, the σ value was used only for the crude concentration estimation of divalent Si because the accuracy has not been tested well.

As described above, 20%–30% systematic uncertainty may still remain in σ for Si-Si bond, E' center, and NBOHC used in this study. On the other hand, statistical error of the measurement of the absorption coefficient was $\sim$0.05 cm^{-1}, indicating that the measurement error was much smaller than the uncertainty in σ. Thus, a conservative error estimate for concentrations of Si-Si bond, E' center, and NBOHC can be set as $\pm$50%. The peak parameters used in this study are summarized in Table I.

The presence of interstitial O_2 is detected by their IR PL band at 1272 nm under excitation at 765 (Ref. 10) or 1064 nm.[77] The excitation efficiency is two orders of magnitude smaller at 1064 nm than at 765 nm. However, the 1064 nm excitation simultaneously induces the fundamental Raman bands of a-SiO_2, which are located spectrally close to the O_2 PL band and have comparable intensities. Thus, the Raman bands can be used as the internal standard of the PL intensity; the concentration of interstitial O_2 can be determined from the PL intensity normalized by the intensity of the Raman bands once the relation is determined.[78] The relation has been calibrated by thermal-desorption spectroscopy, with recording of both the number of thermally desorbed O_2 molecules and the simultaneous decrease in the normalized PL intensity.[47,79] This calibrated relation makes it possible to determine the absolute concentration of interstitial O_2 in standard "reference" samples within $\pm$20%.[47] The statistical error of the O_2 concentration measurement relative to such precalibrated reference sample under excitation at 765 nm was within $\sim$5%. Another potential source of error, the variation in the PL quantum yield, is negligibly small when the concentration of SiOH groups is less than $\sim 2\times10^{18}$ cm^{-3}.[80]

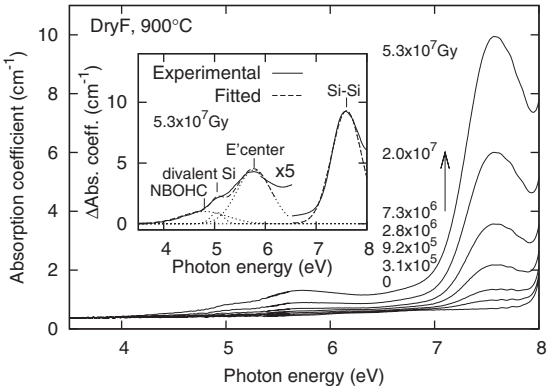

FIG. 1. Optical absorption spectra (resolution of 1 nm) of the DryF samples heated at 900 °C and irradiated with ^{60}Co γ rays. The inset shows the induced absorption spectra at a cumulative dose of $\sim 5.3\times10^7$ Gy, obtained by subtracting the spectrum of the unirradiated sample from the original spectrum. The induced absorption spectrum is fitted with a linear combination of Gaussian-shaped bands of NBOHC, divalent Si, E' center, and Si-Si bond by least-squares fitting. The peak parameters used for the fitting is listed in Table I.

III. RESULTS

Figure 1 shows optical-absorption spectra of the DryF sample annealed at 900 °C followed by γ-ray irradiation up to $\sim 5.3\times10^7$ Gy, and the inset shows the peak decomposition of the induced absorption. The largest peak located at 7.6 eV was caused by Si-Si bonds. The induced absorption below 6 eV was simulated well with a linear combination of three bands associated with NBOHC (peak position, 4.8 eV), divalent Si (5.05 eV), and E' center (5.78 eV). However, it was not possible to decompose the induced absorption between 6 and 7 eV because in this region the parameters of absorption bands are presently not accurately known. The concentrations of NBOHC, E' center, and Si-Si bond were calculated using the σ values listed in Table I. The contribution of divalent Si was minor; the concentration of divalent Si was 1–2 orders of magnitude smaller than that of Si-Si bond.[81] Figure 2 shows the induced absorption and interstitial O_2 PL spectra for the DryF samples preannealed at 900 and 1400 °C. The induced absorption and PL bands were stronger in the sample annealed at 1400 °C.

Figure 3 summarizes the variation in the defect concentrations with the γ-ray dose D. In the DryF sample [Fig. 3(a)], Si-Si bond was the most abundant defect species, even when considering the maximum uncertainty of the defect concentration [$\pm$50% (see Sec. II B)]. The slopes of the plots for Si-Si bond and interstitial O_2 were close to one at small D, indicating a linear concentration dependence on D. However, the slopes gradually decreased with an increase in D. In contrast, the concentrations of E' centers and NBOHCs were

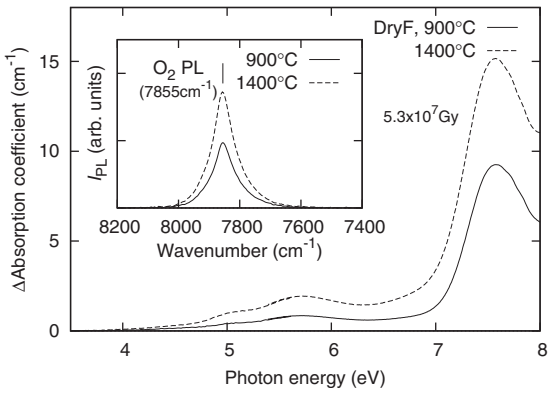

FIG. 2. Induced optical-absorption spectra of the DryF samples preannealed at 900 or 1400 °C and exposed to $\sim 5.3\times10^7$ Gy γ rays. The inset shows IR PL spectra of interstitial O_2 excited at 765 nm.

nearly equal within their uncertainties, and increased sublinearly with D (average slope: $\sim$0.5–0.6) even at small D, consistent with earlier reports on defect formation in γ-ray-irradiated a-SiO_2.[2,6,31] The defect concentrations in the samples annealed at 1400 °C were larger than those in the samples annealed at 900 °C. In addition, the ratio r between the defect concentrations in the 1400 and 900 °C samples was nearly constant at each D, leading to a parallel upward shift of the logarithmic plots with higher temperature annealing. The shift was larger for the dangling bonds than for the Frenkel defects; the average r values were $\sim$2.6 for E' center, $\sim$2.8 for NBOHC, $\sim$1.8 for Si-Si bond, and $\sim$1.9 for interstitial O_2.

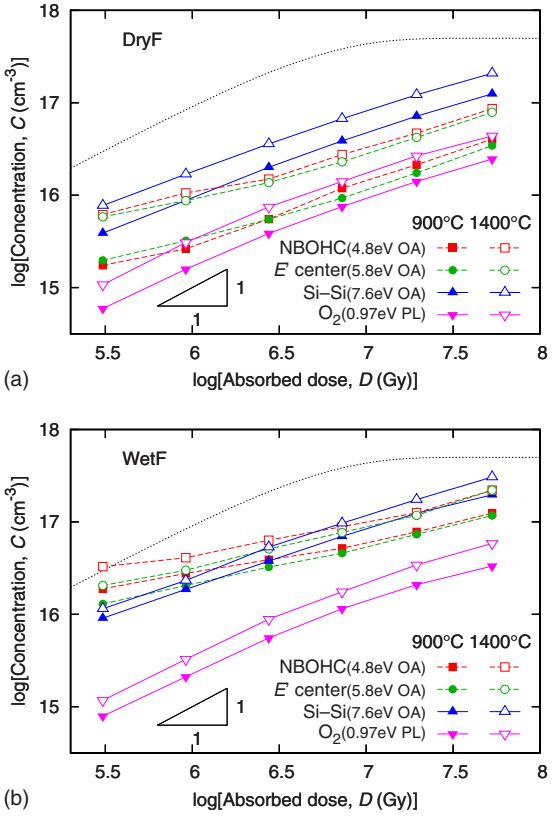

FIG. 3. (Color online) Variations in concentrations C of NBOHC, E' center, Si-Si bond, and interstitial O_2 with γ-ray absorbed dose D (SiO_2 equivalent) in the (a) DryF and (b) WetF samples annealed at 900 or 1400 °C. The dotted lines illustrate theoretical curves calculated at semiarbitrarily chosen values of the formation rate (5×10^{11} cm^{-3} Gy^{-1}) and equilibrium concentration (5×10^{17} cm^{-3}). The theoretical curve represents the single exponential defect formation kinetics and the derivation is described in the Appendix.

The concentrations of defects in the WetF sample [Fig. 3(b)] were larger than those in the DryF sample [Fig. 3(a)]. The formation of NBOHC in larger numbers than that of E' center at small D was evidently due to the radiolysis of SiO-H bonds.[28,29] The concentration of interstitial O_2 depended linearly on D at small D similar to the case for the DryF sample. However, the ratio between the concentrations of Si-Si bond and interstitial O_2 decreased with D, exhibiting an excess formation of Si-Si bonds at low D in the WetF sample. This process is probably due to the photochemical reduction in Si-O-Si bond with interstitial H_2 under electronic excitation,[82]

$$\equiv \text{Si-O-Si} \equiv + H_2 \xrightarrow{h\nu} \equiv \text{Si-Si} \equiv + H_2O, \tag{4}$$

where interstitial H_2 is generated by the dimerization of hydrogen atoms created from SiOH groups.[28,29] The average r values (E' center, $\sim$1.6; NBOHC, $\sim$1.7; Si-Si bond, $\sim$1.4; interstitial O_2, $\sim$1.6) were smaller than those measured in the DryF sample. Nevertheless, despite these small differences, the general tendencies of the defect formations in the DryF and WetF samples were similar, indicating that the presence of $\sim10^{18}$ cm^{-3} of SiOH groups does not change the main defect formation mechanism. It is noteworthy that the initial slope for interstitial O_2 was $\sim$1 in all the samples and thus interstitial O_2 is useful in monitoring the reaction [Eq. (2)].

Since the concentrations of Si-Si bonds and interstitial O_2 depend linearly on D at small D, the formation yield Φ may be calculated as

$$\Phi = \frac{C}{N} = \frac{C}{D\rho/W}, \tag{5}$$

where N and C are the densities of radiation-induced electron-hole pairs and created defects, respectively, ρ is the density of a-SiO_2 ($\rho \simeq 2.2$ g cm^{-3}),[83] and W is the energy required to generate an electron-hole pair. Table II summarizes the C/D values derived from the plots shown in Fig. 3, and the Φ values calculated at $W=18$ eV.[84] The formation yield of Si-Si bonds agrees well with that in a-SiO_2 subjected to electronic excitation with 10 MeV protons [$\Phi \simeq 1\times10^{-5}$ at $W=18$ eV (Ref. 9)].

IV. DISCUSSION

An important finding in this study is that Si-Si bond emerges as the main intrinsic γ-ray induced defect if the extrinsic defect precursors are eliminated. The concentrations of Si-Si bond and interstitial O_2 depend linearly on dose D at small D. The concentration of interstitial O_2 being

TABLE II. Initial concentration to dose ratio C/D (cm^{-3} Gy^{-1}, at $D<10^6$ Gy) and quantum yield Φ of the formation of Si-Si bond and interstitial O_2 by γ-ray irradiation. C/D is obtained as the C intercept of the linear extrapolation of the plots at $D<10^6$ Gy in Fig. 3. Φ is calculated from C/D using Eq. (5) on assumption that the average energy required to form an electron-hole pair in a-SiO_2 is 18 eV (Ref. 84).

		Si-Si bond		Interstitial O_2	
Sample		C/D	Φ	C/D	Φ
DryF	900 °C	1.1×10^{10}	1×10^{-5}	1.8×10^{9}	2×10^{-6}
	1400 °C	2.2×10^{10}	3×10^{-5}	3.4×10^{9}	5×10^{-6}
WetF	900 °C	2.5×10^{10}	3×10^{-5}	2.4×10^{9}	3×10^{-6}
	1400 °C	3.1×10^{10}	4×10^{-5}	3.7×10^{9}	5×10^{-6}

less than that predicted by the mechanism Eq. (2) indicates that only O^0s created as close pairs are dimerized.[85] The concentrations of E' center and NBOHC are nearly equal at all D, suggesting that their main formation mechanism is Eq. (1). However, they are less than the concentration of Si-Si bonds and even less than the lower concentration limit of radiation-induced O^0s given by twice the O_2 concentration at large D in the DryF sample. Thus, we conclude that the Frenkel mechanism [Eq. (2)] is the main intrinsic defect process in a-SiO_2 subjected to band-to-band electronic excitation.

The significant difference in the defect concentration between the samples preannealed at 900 or 1400 °C (Fig. 3), which have different concentrations of "frozen-in" strained Si-O-Si bonds, provides an additional insight into their role in defect formation. The enhanced creation of the dangling bonds in the sample annealed at higher temperature demonstrates that the dangling bonds are generated mainly from the strained bonds, in accord with the previous reports.[2,5,7] An important finding is that the "defect enhancement factor" r remains nearly constant at all investigated Ds, even at the largest D, indicating that the strained bonds remain the dominant dangling-bond precursors at all Ds and the contributions from the much more abundant precursor sites in the form of "normal," nonstrained Si-O-Si bonds (4.4×10^{22} cm^{-3}) are relatively insignificant.

While the correlation between the strained bond precursors and radiation-induced dangling bonds in a-SiO_2 is predictable, a similar effect on the creation of the Frenkel defects is intuitively less obvious. The present data demonstrate that the formation of Si-Si bonds and interstitial O_2 is indeed enhanced by increasing the preannealing temperature from 900 to 1400 °C. This result shows that the strained bonds are also the main precursor sites for the Frenkel process [Eq. (2)]. Indeed, in α-quartz in which Si-O-Si bonds are relaxed, γ irradiation creates Si-Si bonds with much lower efficiency[86] and does not form detectable interstitial O_2.[10] Thus, it is most likely that the strained bonds enhance the localization of excitation energy, and the conversion to persistent defects via Eqs. (1) and (2).

The kinetics of the reaction mechanisms described by Eqs. (1) and (2) is single exponential when each precursor site has the same Φ value (see the Appendix and Fig. 4). Typical theoretical curves for such exponential defect formation kinetics are shown as dotted lines in Fig. 3. The slope of the theoretical curves changes sharply from one to zero near the equilibrium concentration. Their character is not much changed by taking first- or second-order back reaction into account. In contrast, the slopes for the observed curves decrease gradually with D probably because of an overlap of processes characterized by different Φ values, as shown in Fig. 4(b). The transition range widens with an increase in the Φ distribution width, resulting in a sublinear concentration

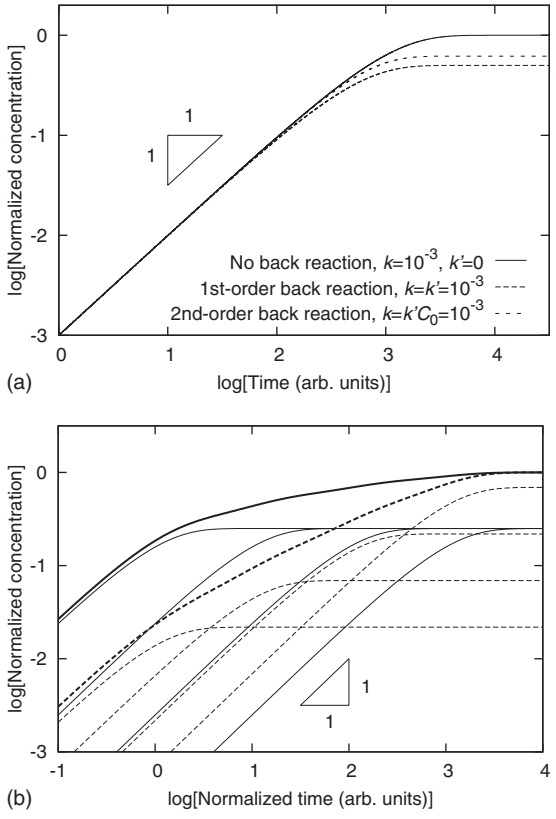

FIG. 4. (a) Typical simulated curves of time-dependent change in normalized concentration of products A_1 and A_2 generated by the mechanism [Eq. (A1)]. Curves for no [$k'=0$ in Eq. (A3)], first-order [$k'=k$ in Eq. (A3)], and second-order [$k'=k/C_0$ in Eq. (A6)] backward reactions are drawn at $k=10^{-3}$. (b) Effect of overlap of defect formation processes of different time constants τ. Each τ component is shown with thin lines. Two examples, where the saturation concentration of the components is constant and increases with τ (solid and dashed lines, respectively), are exhibited. In the total concentration changes (thick lines), sublinear concentration dependence on time is clearly seen.

increase over a wide D range. The difference in Φ may originate from the site to site structural variation of the local configuration of the defect precursors. A similar idea has been put forward to explain the sublinear dose dependence of photoinduced compaction of a-SiO_2.[87] Thus, the slopes for the E' center and NBOHC plots being less than those of the Si-Si bond and interstitial O_2 plots suggest that Φ of the dangling-bond pair is more sensitive to the local Si-O-Si configuration. Indeed, as shown by larger r values for the dangling bonds ($\sim$2.7) than for the vacancy interstitials ($\sim$1.9), the dangling-bond mechanism is more susceptible to the degree of the structural disorder of a-SiO_2 than the Frenkel mechanism.

V. CONCLUSIONS

The present paper reports three fundamental findings on intrinsic defect formation in a-SiO_2: (i) The Frenkel process, which is the main intrinsic defect formation mechanism in crystalline solids, is also the main process in a-SiO_2, prevailing over the bond dissociation mechanism specific to the amorphous state. (ii) The efficiency of the Frenkel process is influenced by the degree of structural disorder (distribution in the Si-O-Si angle) of a-SiO_2, making the process dependent on the fictive temperature and rendering it much more efficient in a-SiO_2 than in α-quartz. (iii) The structural disorder enhances the bond dissociation mechanism more strongly than the Frenkel mechanism.

ACKNOWLEDGMENT

The ^{60}Co γ-ray irradiation was performed at the Cobalt 60 Irradiation Facilities of the Takasaki Advanced Radiation Research Institute, under the Common-Use Facility Program of Japan Atomic Energy Agency (JAEA).

APPENDIX

Defect formation from precursor A (initial concentration C_0) into defect pair A_1 and A_2 (concentrations C; $C=0$ at time zero $t=0$) will be considered. This process may consist of forward and backward reactions as

$$A \rightleftarrows A_1 + A_2. \tag{A1}$$

It is assumed that the forward reaction is first order and the rate constant is k.

When the back reaction is first order (rate constant k'), the rate equation for the products A_1 and A_2 is given by

$$\frac{dC}{dt} = -k'C + k(C_0 - C) = -(k' + k)C + kC_0, \tag{A2}$$

$$C = \frac{kC_0}{k+k'}\exp(-t/\tau) \quad \text{where} \quad \tau^{-1} = k + k'. \tag{A3}$$

Thus, the reaction kinetics is single exponential irrespective of the rate of the backward reaction.

When the backward reaction is second order ($k' \neq 0$), the rate equation becomes

$$\frac{dC}{dt} = -k'C^2 + k(C_0 - C) = -k'(C-\alpha)(C-\beta),$$

$$\text{where} \quad \alpha,\beta(\alpha > \beta) = \frac{-k/k' \pm \sqrt{(k/k')^2 + 4kC_0/k'}}{2}. \tag{A4}$$

The definite integration of Eq. (A4) yields

$$\frac{C-\alpha}{C-\beta} = \frac{\alpha}{\beta}\exp(-t/\tau),$$

$$\text{where} \quad \tau^{-1} = k'(\alpha - \beta) = \sqrt{k^2 + 4kk'C_0}. \tag{A5}$$

The rearrangement of Eq. (A5) gives

$$C = \frac{\alpha[1 - \exp(-t/\tau)]}{1 - \alpha\exp(-t/\tau)/\beta}. \tag{A6}$$

The value $-\alpha/\beta$ is a monotonic function of k'/k that is expressed by

$$-\frac{\alpha}{\beta} = \frac{\sqrt{4C_0k'/k+1} - 1}{\sqrt{4C_0k'/k+1} + 1}. \tag{A7}$$

Since $-\alpha/\beta$ takes the maximum value of one at $C_0k'/k \gg 1$ (case back reaction is faster than the forward reaction) and the minimum value of zero at $C_0k'/k \ll 1$ (case backward reaction does not occur or is very slow), the denominator of Eq. (A6) ranges only between one and two. Furthermore, the term $\alpha\exp(-t/\tau)/\beta$ approaches zero with an increase in t. Thus, Eq. (A6) is approximately described by the single exponential kinetics as

$$C \simeq \alpha[1 - \exp(-t/\tau)]. \tag{A8}$$

Typical t-C relations of Eqs. (A3) and (A6) are shown in Fig. 4(a). It is evident that the shape of the t-C curve is almost irrelevant to the rate and order of the backward reaction. These results indicate that these simple models do not explain the sublinear time (dose) dependence of the defect concentration.

Figure 4(b) shows that the sublinear time dependence can be reproduced by an overlap of processes with different time constants τ.

*Author to whom correspondence should be addressed. kkaji@tmu.ac.jp

[1] N. Itoh and A. M. Stoneham, *Materials Modification by Electronic Excitation* (Cambridge University Press, Cambridge, England, 2001).

[2] R. A. B. Devine and J. Arndt, Phys. Rev. B **39**, 5132 (1989).

[3] R. A. B. Devine and J. Arndt, Phys. Rev. B **42**, 2617 (1990).

[4] K. Arai, H. Imai, J. Isoya, H. Hosono, Y. Abe, and H. Imagawa, Phys. Rev. B **45**, 10818 (1992).

[5] F. L. Galeener, D. B. Kerwin, A. J. Miller, and J. C. Mikkelsen, Jr., Phys. Rev. B **47**, 7760 (1993).

[6] H. Imai, K. Arai, J. Isoya, H. Hosono, Y. Abe, and H. Imagawa, Phys. Rev. B **48**, 3116 (1993).

[7] H. Hosono, Y. Ikuta, T. Kinoshita, K. Kajihara, and M. Hirano, Phys. Rev. Lett. **87**, 175501 (2001).

[8] T. E. Tsai and D. L. Griscom, Phys. Rev. Lett. **67**, 2517 (1991).

[9] H. Hosono, H. Kawazoe, and N. Matsunami, Phys. Rev. Lett. **80**, 317 (1998).

[10] L. Skuja, B. Güttler, D. Schiel, and A. R. Silin, Phys. Rev. B **58**, 14296 (1998).

[11] M. A. Stevens-Kalceff, Phys. Rev. Lett. **84**, 3137 (2000).

[12] R. A. Weeks, J. Appl. Phys. **27**, 1376 (1956).

[13] E. W. J. Mitchell and E. G. S. Paige, Philos. Mag. **1**, 1085 (1956).

[14] A. J. Fisher, W. Hayes, and A. M. Stoneham, Phys. Rev. Lett. **64**, 2667 (1990).

[15] A. Shluger and E. Stefanovich, Phys. Rev. B **42**, 9664 (1990).

[16] T. Uchino and T. Yoko, Phys. Rev. B **68**, 041201(R) (2003).

[17] D. Donadio and M. Bernasconi, Phys. Rev. B **71**, 073307 (2005).

[18] C. Itoh, T. Suzuki, and N. Itoh, Phys. Rev. B **41**, 3794 (1990).

[19] K. Awazu and H. Kawazoe, J. Appl. Phys. **94**, 6243 (2003).

[20] M. Yamaguchi, K. Saito, and A. J. Ikushima, Phys. Rev. B **68**, 153204 (2003).

[21] D. L. Griscom, J. Non-Cryst. Solids **352**, 2601 (2006).

[22] W. Hayes and T. J. L. Jenkin, J. Phys. C **19**, 6211 (1986).

[23] K. Tanimura, T. Tanaka, and N. Itoh, Phys. Rev. Lett. **51**, 423 (1983).

[24] C. Itoh, K. Tanimura, and N. Itoh, J. Phys. C **21**, 4693 (1988).

[25] Formation of dangling bonds in α-quartz irradiated with neutron, electron, and heavy-ion beams is mostly related to radiation-induced amorphization. Other cases of creation of dangling bonds (E' centers) can be explained by the decomposition of oxygen vacancies and impurities.

[26] F. Messina and M. Cannas, J. Phys.: Condens. Matter **18**, 9967 (2006).

[27] L. Skuja, K. Kajihara, M. Hirano, and H. Hosono, Nucl. Instrum. Methods Phys. Res. B **266**, 2971 (2008).

[28] D. L. Griscom, J. Non-Cryst. Solids **68**, 301 (1984).

[29] K. Kajihara, L. Skuja, M. Hirano, and H. Hosono, Phys. Rev. B **74**, 094202 (2006).

[30] K. Kajihara, L. Skuja, M. Hirano, and H. Hosono, Appl. Phys. Lett. **79**, 1757 (2001).

[31] L. Vaccaro, M. Cannas, B. Boizot, and A. Parlato, J. Non-Cryst. Solids **353**, 586 (2007).

[32] D. L. Griscom and E. J. Friebele, Phys. Rev. B **34**, 7524 (1986).

[33] D. L. Griscom, in *Defects in SiO_2 and Related Dielectrics: Science and Technology*, NATO Science Series II: Mathematics, Physics and Chemistry, edited by G. Pacchioni, L. Skuja, and D. L. Griscom (Kluwer Academic, Dordrecht, 2000), pp. 117–159; see Ref. 88.

[34] C. M. Nelson and R. A. Weeks, J. Appl. Phys. **32**, 883 (1961).

[35] E. P. O'Reilly and J. Robertson, Phys. Rev. B **27**, 3780 (1983).

[36] H. Imai, K. Arai, H. Imagawa, H. Hosono, and Y. Abe, Phys. Rev. B **38**, 12772 (1988).

[37] R. Tohmon, H. Mizuno, Y. Ohki, K. Sasagane, K. Nagasawa, and Y. Hama, Phys. Rev. B **39**, 1337 (1989).

[38] H. Hosono, Y. Abe, H. Imagawa, H. Imai, and K. Arai, Phys. Rev. B **44**, 12043 (1991).

[39] M. Guzzi, M. Martini, A. Paleari, F. Pio, A. Vedda, and C. B. Azzoni, J. Phys. C **5**, 8105 (1993).

[40] K. Kajihara, L. Skuja, M. Hirano, and H. Hosono, Phys. Rev. Lett. **92**, 015504 (2004).

[41] K. Kajihara, M. Hirano, L. Skuja, and H. Hosono, Chem. Lett. **36**, 266 (2007).

[42] K. Awazu, H. Kawazoe, and K. Muta, J. Appl. Phys. **69**, 4183 (1991).

[43] H. Hosono, M. Mizuguchi, H. Kawazoe, and T. Ogawa, Appl. Phys. Lett. **74**, 2755 (1999).

[44] E. Dooryhée, J. P. Duraud, and R. A. B. Devine, in *Structure and Imperfections in Amorphous and Crystalline Silicon Dioxide*, edited by R. A. B. Devine, J. P. Duraud, and E. Dooryhée (Wiley, Chichester, England, 2000), pp. 349–421.

[45] SiCl groups and interstitial H_2 were below detection limit ($\lesssim 10^{17}$ cm^{-3}) in all the samples.

[46] 1 Gy is defined as 1 J kg^{-1}. The absorbed dose rate $\sim 1.3 \times 10^4$ Gy h^{-1} corresponds to an exposure dose rate $\sim 3.9 \times 10^2$ C kg^{-1} h^{-1} or $\sim 1.5 \times 10^6$ R h^{-1}.

[47] K. Kajihara, T. Miura, H. Kamioka, A. Aiba, M. Uramoto, Y. Morimoto, M. Hirano, L. Skuja, and H. Hosono, J. Non-Cryst. Solids **354**, 224 (2008).

[48] The conversion between f and σ was done using Smakula's equation with the Onsager effective-field correction $\alpha f = 9.111 \times 10^{15} \Omega\, \sigma (2n^2+1)^2/(9n^3)$, where Ω is the integral of the absorption spectrum and α is the peak absorption coefficient. For more details refer to, e.g., Ref. 69. The refractive index n was taken from Ref. 89.

[49] J. E. Shelby, J. Appl. Phys. **50**, 3702 (1979).

[50] G. Pacchioni and G. Ieranó, Phys. Rev. B **57**, 818 (1998).

[51] U. Itoh, Y. Toyoshima, H. Onuki, N. Washida, and T. Ibuki, J. Chem. Phys. **85**, 4867 (1986).

[52] B. B. Stefanov and K. Raghavachari, Phys. Rev. B **56**, 5035 (1997).

[53] S. Mukhopadhyay, P. V. Sushko, A. M. Stoneham, and A. L. Shluger, Phys. Rev. B **71**, 235204 (2005).

[54] Y. Morimoto, T. Igarashi, H. Sugahara, and S. Nasu, J. Non-Cryst. Solids **139**, 35 (1992).

[55] B. C. Schmidt, F. M. Holtz, and J.-M. Beny, J. Non-Cryst. Solids **240**, 91 (1998).

[56] C. M. Nelson and R. A. Weeks, J. Am. Ceram. Soc. **43**, 396 (1960).

[57] R. A. Weeks and E. Sonder, in *Paramagnetic Resonance*, edited by W. Low (Academic, New York, 1963), Vol. 2, pp. 869–879.

[58] H. Nishikawa, E. Watanabe, D. Ito, and Y. Ohki, J. Non-Cryst. Solids **179**, 179 (1994).

[59] G. Buscarino, R. Boscaino, S. Agnello, and F. M. Gelardi, Phys. Rev. B **77**, 155214 (2008).

[60] R. Boscaino, M. Cannas, F. M. Gelardi, and M. Leone, Nucl. Instrum. Methods Phys. Res. B **116**, 373 (1996).

[61] We calculated the value from the data shown in Ref. 57: point 2 in Fig. 2 (relying on the linear relation the corrected absorption

coefficient of 75 cm^{-1} was used) and the corresponding spin concentration in Table II (2.22×10^{18} cm^{-3}).
[62] Calculated from data shown in Fig. 1 in Ref. 60.
[63] Calculated from data shown in Fig. 3(d) in Ref. 59 at FWHM =0.6 eV.
[64] G. Pacchioni, G. Ieranò, and A. M. Márquez, Phys. Rev. Lett. **81**, 377 (1998).
[65] M. Stapelbroek, D. L. Griscom, E. J. Friebele, and G. H. Sigel, Jr., J. Non-Cryst. Solids **32**, 313 (1979).
[66] V. A. Radtsig and A. B. Bistrikov, Kinet. Katal. **19**, 713 (1978).
[67] L. Skuja, J. Non-Cryst. Solids **179**, 51 (1994).
[68] L. Skuja, M. Hirano, H. Hosono, K. Kajihara, and A. Silin, Glastech. Ber. Glass Sci. Technol. (Offenbach, Ger.) **75C**, 24 (2002).
[69] L. Skuja, in *Defects in SiO_2 and Related Dielectrics: Science and Technology*, NATO Science Series II: Mathematics, Physics and Chemistry, edited by G. Pacchioni, L. Skuja, and D. L. Griscom (Kluwer Academic, Dordrecht, 2000), pp. 73–116; see Ref. 88.
[70] L. Vaccaro, M. Cannas, and R. Boscaino, Solid State Commun. **146**, 148 (2008).
[71] L. Skuja (unpublished).
[72] L. Skuja, K. Kajihara, M. Hirano, and H. Hosono, Proceedings of the 20th International Congress on Glass, 2004, p. O-14-052.
[73] L. Skuja, K. Kajihara, M. Hirano, A. Saitoh, and H. Hosono, J. Non-Cryst. Solids **352**, 2297 (2006).
[74] H. Nishikawa, E. Watanabe, D. Ito, and Y. Ohki, Phys. Rev. Lett. **72**, 2101 (1994).
[75] L. N. Skuja, A. N. Streletsky, and A. B. Pakovich, Solid State Commun. **50**, 1069 (1984).
[76] R. Boscaino, M. Cannas, F. M. Gelardi, and M. Leone, Phys. Rev. B **54**, 6194 (1996).
[77] L. Skuja and B. Güttler, Phys. Rev. Lett. **77**, 2093 (1996).
[78] L. Skuja, B. Güttler, D. Schiel, and A. R. Silin, J. Appl. Phys. **83**, 6106 (1998).
[79] K. Kajihara, M. Hirano, M. Uramoto, Y. Morimoto, L. Skuja, and H. Hosono, J. Appl. Phys. **98**, 013527 (2005).
[80] K. Kajihara, H. Kamioka, M. Hirano, T. Miura, L. Skuja, and H. Hosono, J. Appl. Phys. **98**, 013528 (2005).
[81] Estimation based on the observation that the ratio of the peak amplitudes of the 7.6 and 5.0 eV OA bands was ~30–60. The presence of divalent Si was confirmed by the characteristic 4.4 and 2.7 eV PL bands.
[82] Y. Ikuta, K. Kajihara, M. Hirano, S. Kikugawa, and H. Hosono, Appl. Phys. Lett. **80**, 3916 (2002).
[83] R. Brückner, J. Non-Cryst. Solids **5**, 123 (1970).
[84] G. A. Ausman, Jr. and F. B. McLean, Appl. Phys. Lett. **26**, 173 (1975).
[85] The most probable form of the unreacted O^0 is peroxy linkage ≡SiOOSi≡.
[86] L. Skuja, M. Hirano, K. Kajihara, and H. Hosono, Phys. Chem. Glasses **43C**, 145 (2002).
[87] F. Piao, W. G. Oldham, and E. E. Haller, J. Appl. Phys. **87**, 3287 (2000).
[88] *Defects in SiO_2 and Related Dielectrics: Science and Technology*, NATO Science Series II: Mathematics, Physics and Chemistry, edited by G. Pacchioni, L. Skuja, and D. L. Griscom (Kluwer Academic, Dordrecht, 2000).
[89] H. R. Philipp, in *Handbook of Optical Constants of Solids*, Handbook Series, edited by E. D. Palik (Academic, Orlando, 1985), p. 749.